

Self-supported cobalt-nickel bimetallic telluride as an advanced catalyst for oxygen evolution reaction

Yu Qi,^{a,b} Zhi Yang,^a Shuai Peng,^a Mitang Wang,^c Jilin Bai,^a Hong Li,^a and Dehua Xiong^{*,a,b}

a. State Key Laboratory of Silicate Materials for Architectures, Wuhan University of Technology, Wuhan 430070, P. R. China

Corresponding author Email: xiongdehua2010@gmail.com (Dehua Xiong)

b. Wuhan National Laboratory for Optoelectronics, Huazhong University of Science and Technology, Wuhan 430074, P. R. China

c. School of Materials Science and Engineering, University of Shanghai for Science and Technology, Shanghai 200093, P. R. China

List of contents:

Experimental.....	S2-S4
Supplementary figures.....	S5-S10
Fig. S1.....	S5
Fig. S2.....	S6
Fig. S3.....	S7
Fig. S4.....	S8
Fig. S5.....	S9
Fig. S6.....	S10
Fig. S7.....	S11
Fig. S8.....	S12
Fig. S9.....	S13
Fig. S10.....	S14
Table. S1.....	S15

Experimental

Reagents

Sodium tellurite (Na_2TeO_3), Nickel chloride hexahydrate ($\text{NiCl}_2 \cdot 6\text{H}_2\text{O}$), hydrazine hydrate ($\text{N}_2\text{H}_4 \cdot \text{H}_2\text{O}$), Potassium hydroxide (KOH). All chemicals used are of analytical grade and were purchased from Sinopharm Chemical Reagent Co., Ltd. Ultrapure water was used throughout the study.

Catalysts preparation

Hydrothermal synthesis of Ni doped CoTe_2

In general, in order to remove the contaminants on the surface of Co foam and increase its hydrophilicity, a piece of Co foam (i. e. $3.0 \times 4.0 \text{ cm}^2$) was cleaned by ultrasonication in 1.0 M HCl for 30 min to remove the surface oxide layer, and successively washed in water and alcohol, and finally dried at 60 °C in vacuum for 30 min. In a typical hydrothermal experiment, 0.443 g sodium tellurite (Na_2TeO_3) was dissolved in 65 mL of deionized (DI) water to form a homogeneous solution by continuous magnetic stirring for 30 min. Subsequently, $\text{NiCl}_2 \cdot 6\text{H}_2\text{O}$ (i. e. 0.10g, 0.20g, 0.30g, 0.40g) was added and magnetic stirring continued for 30 min to form a uniform solution. Then 5.00 ml hydrazine hydrate ($\text{N}_2\text{H}_4 \cdot \text{H}_2\text{O}$) used as reducing agent was added into the above solution. The precursor mixture was stirred for another 30 minutes at room temperature until a homogeneous suspension was formed, and then the solution was loaded into a 100 mL Teflon-lined autoclave reactor where a piece of cleaned Co foam was placed against the wall. Subsequently, the autoclave reactor was sealed, heated to 240 °C (denoted as $\text{Co}@0.1\text{gNiCoTe}_2\text{-240}$, $\text{Co}@0.2\text{gNiCoTe}_2\text{-240}$, $\text{Co}@0.3\text{gNiCoTe}_2\text{-240}$, $\text{Co}@0.4\text{gNiCoTe}_2\text{-240}$) and maintained 20 hours for hydrothermal reaction. Finally, the reactor was naturally cooled down to room temperature. After the hydrothermal processing, the color of Co foam turned to dark black from light grey, suggesting the formation of nickel cobalt bimetallic nanoparticles on the foam surface. The resultant sample was then rinsed successively with DI water and ethanol, and dried at 50 °C for 1 hours. We used the same procedure to prepare

CoTe₂ at 240 °C without the addition of NiCl₂·6H₂O, which is denoted as Co@CoTe₂-240. We further reduced the hydrothermal reaction temperature as a comparative study, including the temperature at 200 and 160 °C.

Structural characterization

The morphology, microstructure, and chemical composition of bare Co, Co@CoTe₂ and Co@Ni_xCo_{1-x}Te₂ electrodes were examined by field-emission scanning electron microscopy (FESEM, FEG Quanta 450) and transmission electron microscopy (TEM, JEOL JEM-2100 operating at 200 keV) equipped with energy-dispersive X-ray spectroscopy (EDX). The crystalline structure of samples was studied by X-ray diffractometry (XRD, PANalytical X'Pert PRO) using Cu K α radiation ($\lambda = 1.540598$ Å) and a PIXcel detector. The surface chemical states of bare Co, Co@CoTe₂ and Co@Ni_xCo_{1-x}Te₂ were analyzed by X-ray photoelectron spectroscopy (XPS, Thermo Escalab 250 Xi), and the C (1s) line (at 284.80 eV) corresponding to the surface adventitious carbon (C–C line bond) has been used as the reference binding energy.

Electrochemical measurements

The OER performance was evaluated by cyclic voltammetry (CV), chronopotentiometry (CP) and electrochemical impedance spectroscopy (EIS) in a three-electrode configuration in 1.0 M KOH (pH = 13.5) using a CS2350H electrochemical workstation (Wuhan Corrtest Instruments Corp., China). A platinum wire and a saturated calomel electrode (SCE) were used as the counter and reference electrodes, respectively. The as-fabricated Co@CoTe₂ and Co@Ni_xCo_{1-x}Te₂ working electrode was directly used as the working electrode, and the active electrode area was kept to 1×1 cm². Cyclic voltammetric (CV) scans were recorded between 1.05 and 1.80 V vs. reversible hydrogen electrode (RHE) at the scan rate of 5 mV s⁻¹. The electrochemical double-layer capacitance (C_{dl}) of each sample was measured given that C_{dl} is positively proportional to the effective surface areas (ESA). C_{dl} can be extracted through CV scans at different rates (from 10 to 100 mV s⁻¹) in the non-faradaic potential window of -0.05 - 0.05 V vs. SCE. All current density values were normalized with respect to the geometrical surface area of the working electrode. For comparison, the

electrocatalytic performance of a bare Co foam was also measured. All CV curves presented in this work are iR-corrected (85%), and the correction was done according to the following equation:

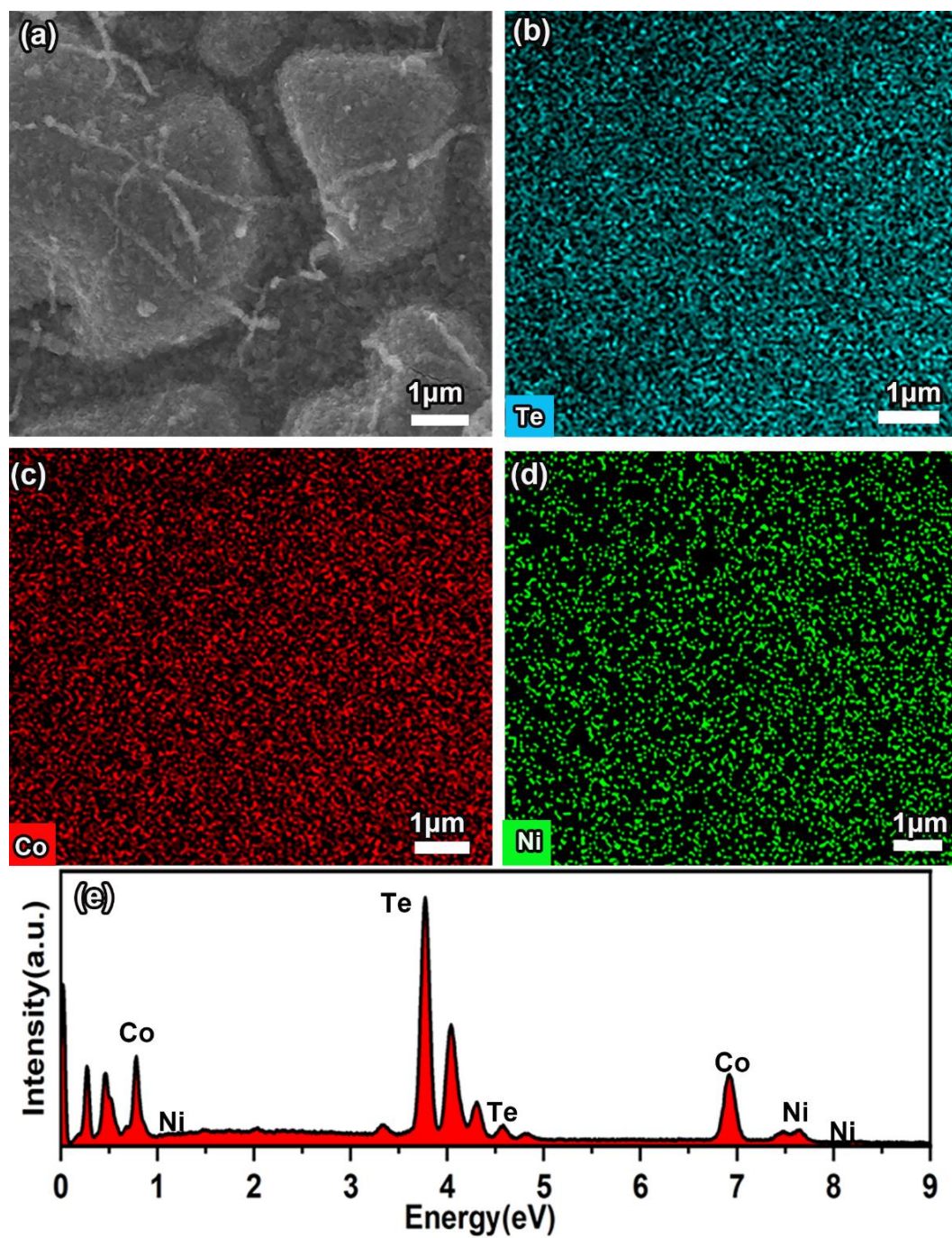
$$E_c = E_m - iR_s$$

where E_c is the iR-corrected potential, E_m experimentally measured potential, and R_s the equivalent series resistance extracted from the electrochemical impedance spectroscopy (EIS) measurements. Unless otherwise specified, all potentials are reported versus reversible hydrogen electrode (RHE) by converting the potentials measured vs. SCE according to the following formula:

$$E(\text{RHE}) = E(\text{SCE}) + 0.241 + 0.059 \text{ pH}$$

The EIS measurements were performed in the frequency range of 10 mHz – 100 kHz under a constant potential of 1.60 V vs. RHE.

Supplementary figures:

Fig. S1. SEM-EDX results of Co@0.2gNiCoTe₂-240 electrode.

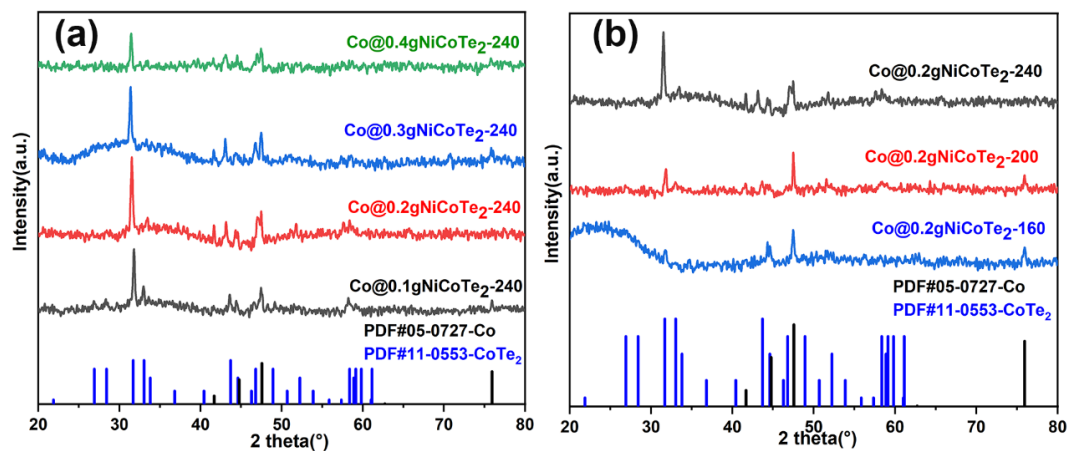


Fig. S2. (a) Different Ni Doping XRD pattern of Ni doped CoTe₂ electrode. (b) Different temperature XRD pattern of Ni_xCo_{1-x}Te₂ electrode. The standard powder diffraction pattern of metallic cobalt and CoTe₂ is given for reference.

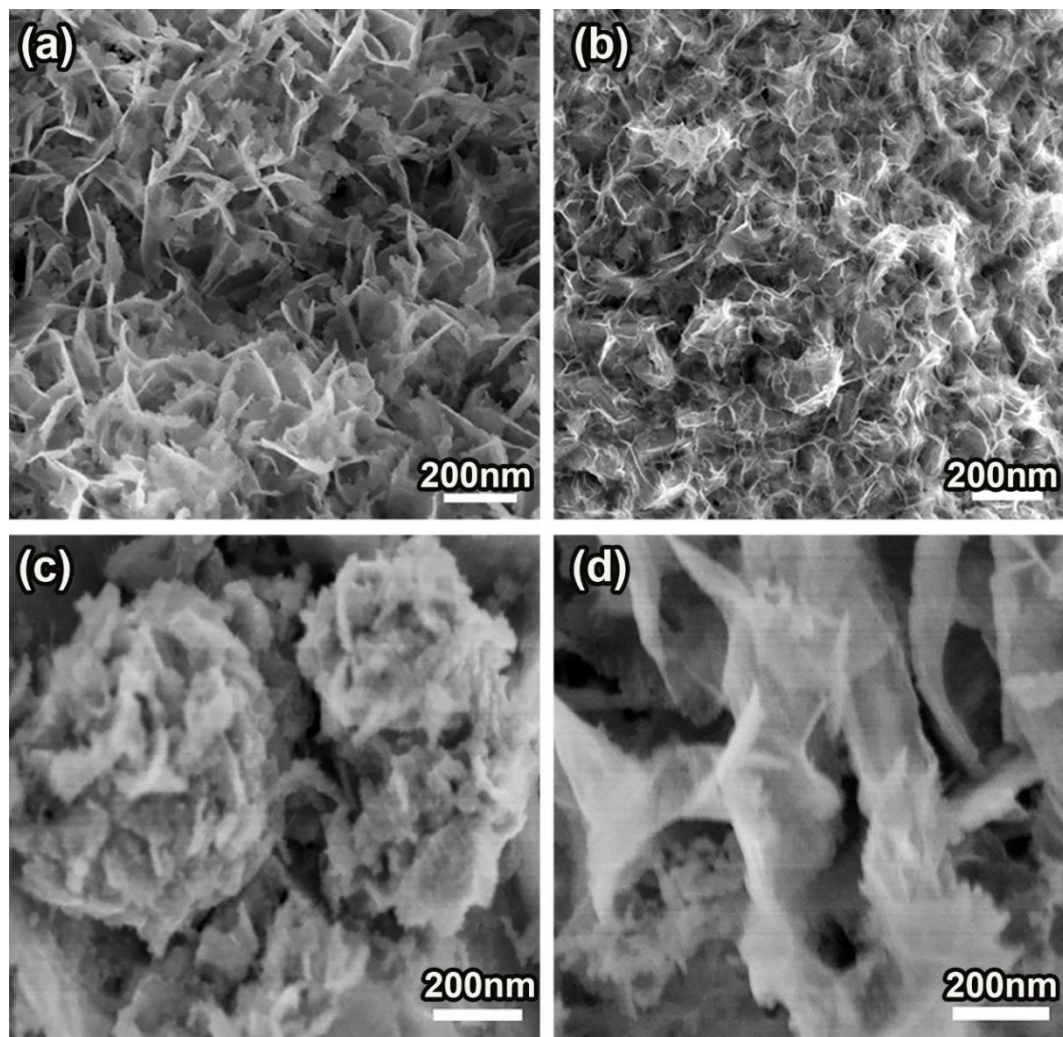


Fig. S3. (a-d) SEM images of Co@0.1g NiCoTe₂-240, Co@0.2g NiCoTe₂-240, Co@0.3gNiCoTe₂-240, Co@0.4gNiCoTe₂-240 electrodes.

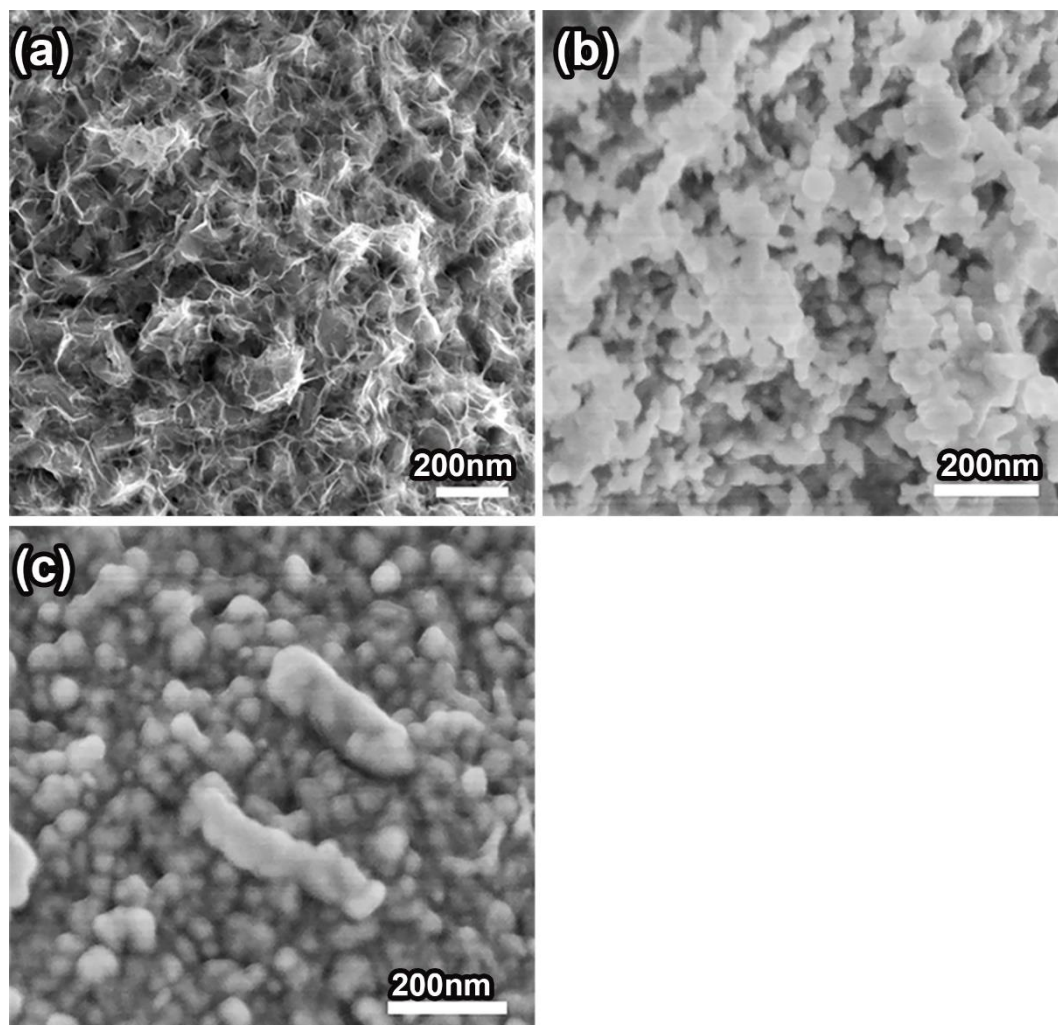


Fig. S4. (a-c) SEM images of Co@0.2gNiCoTe₂-240, Co@0.2gNiCoTe₂-200, Co@0.2gNiCoTe₂-160 electrodes.

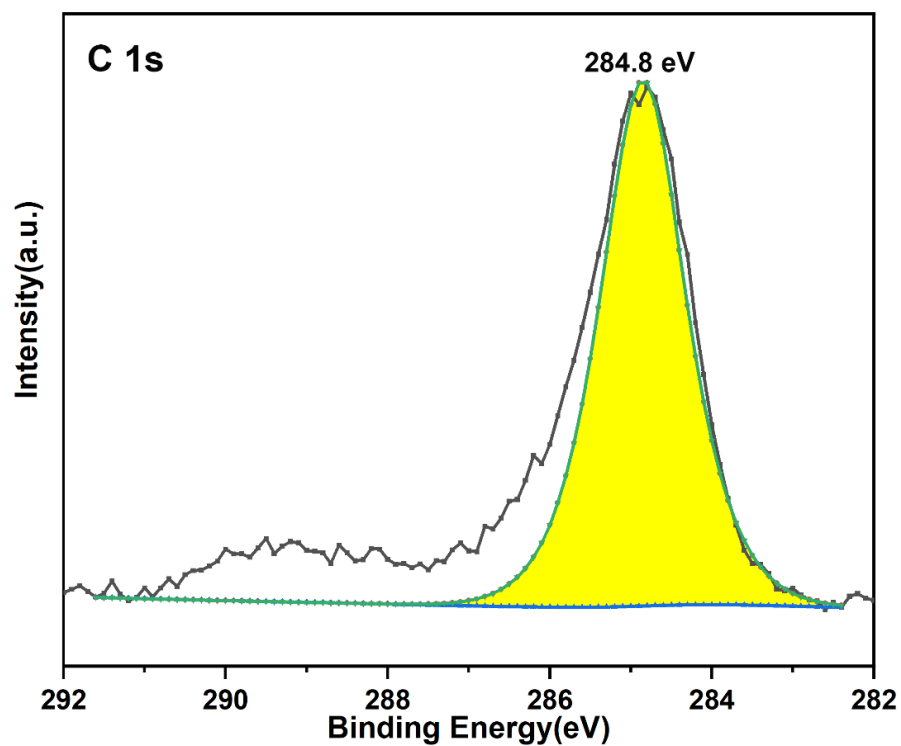


Fig. S5. XPS spectra of C 1s

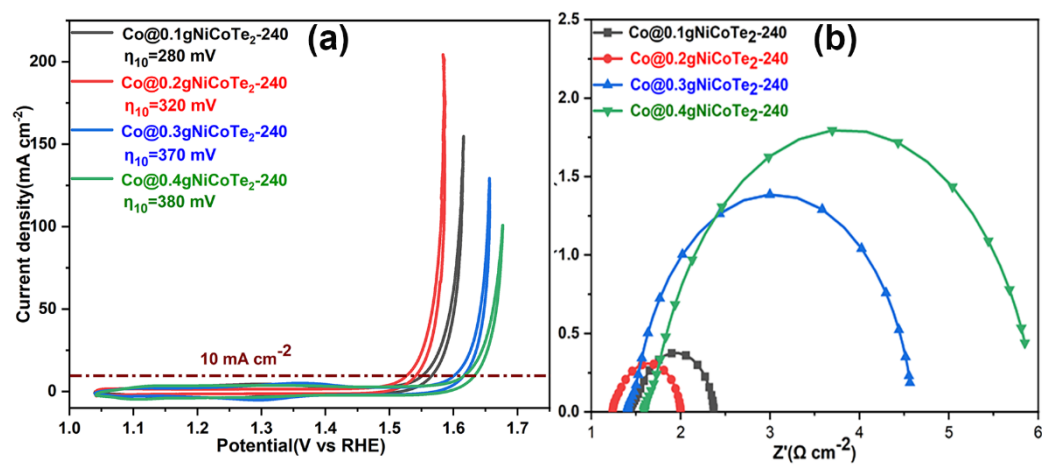


Fig. S6. CV curves (a), and Nyquist plots (b) of the Co@0.1gNiCoTe₂-240, Co@0.2gNiCoTe₂-240, Co@0.3gNiCoTe₂-240 and Co@0.4gNiCoTe₂-240 electrodes;

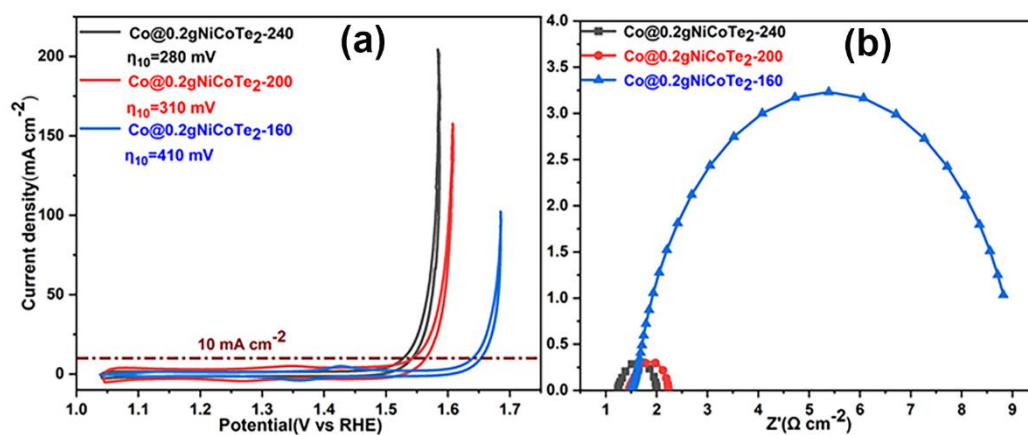


Fig. S7. CV curves (a), and Nyquist plots (b) of the Co@0.2g NiCoTe₂-240, Co@0.2g NiCoTe₂-200 and Co@0.2g NiCoTe₂-160 electrodes.

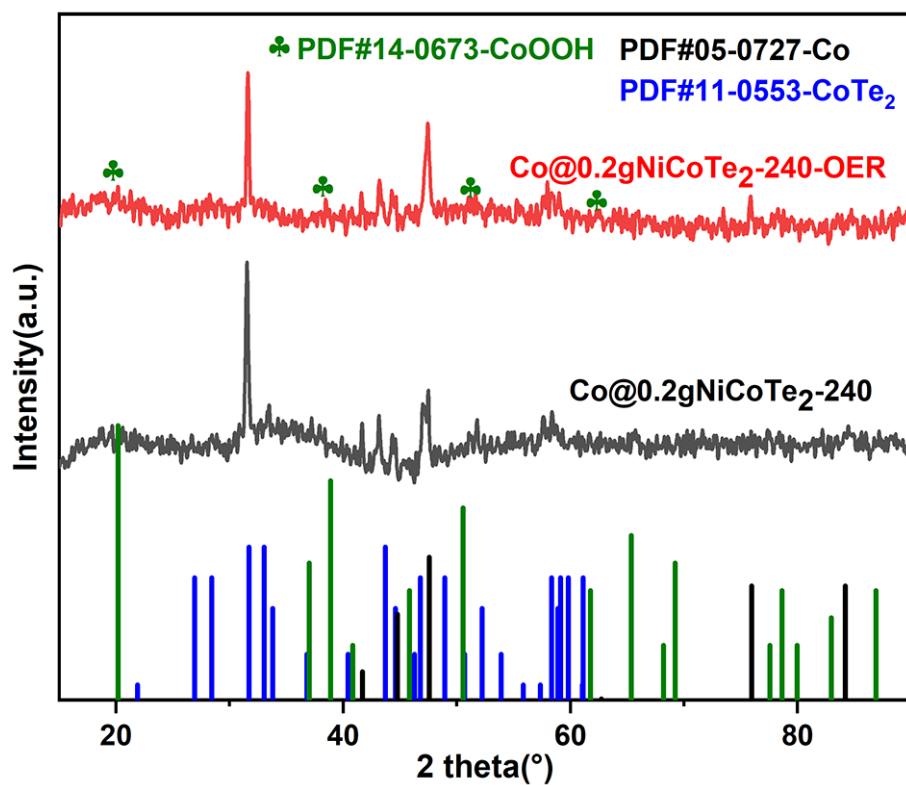


Fig. S8. XRD patterns of the Co@0.2gNiCoTe₂-240 electrode before and after the long-term stability test for 18 hours under OER conditions.

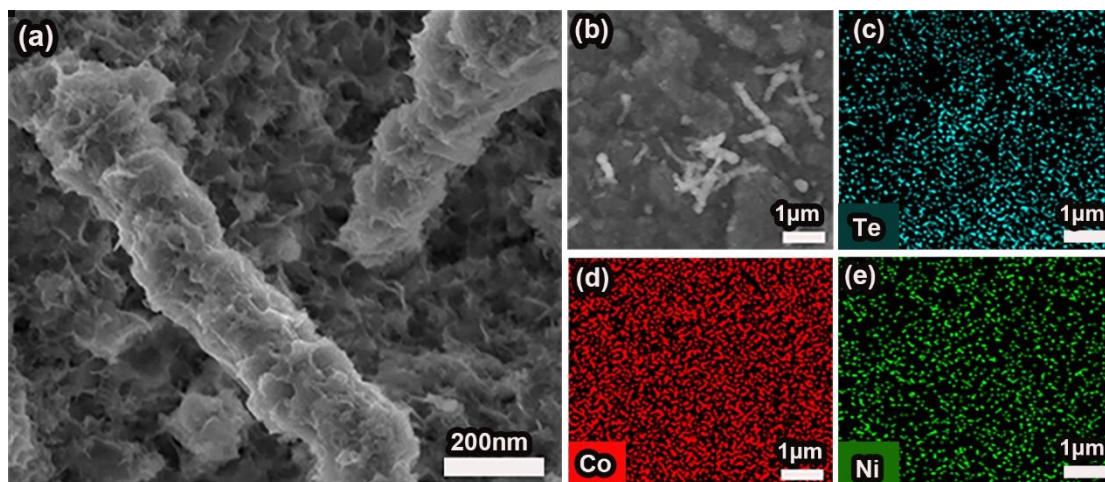


Fig. S9. SEM images (a and b), elemental maps (c, Te; d, Co and e, Ni) for the Co@0.2gNiCoTe₂-240 electrode obtained after 18 hours of continuous chronopotentiometric tests.

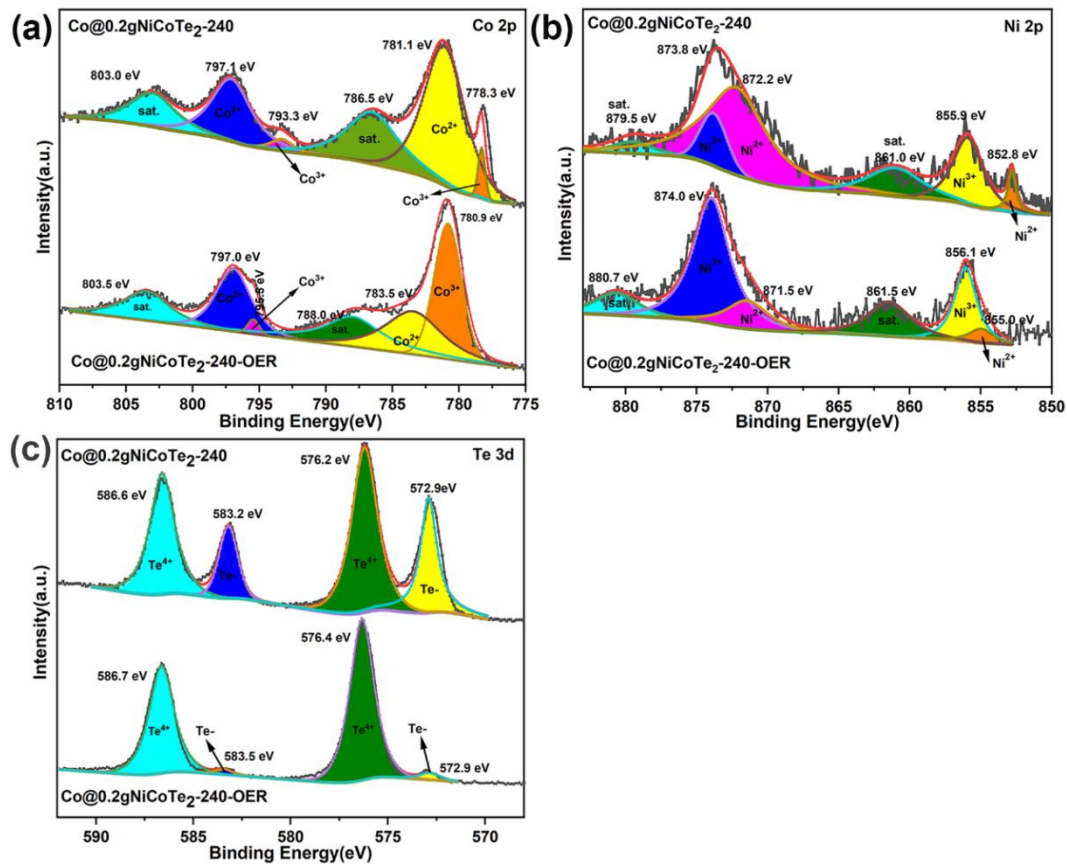


Fig. S10. XPS spectra of (a) Co 2p, (b) Ni 2p, (c) Te 3d for Co@0.2gNiCoTe₂-240 electrode obtained before and after 18 hours of continuous chronopotentiometric tests.

Table S1. Comparison of electrocatalytic parameters of Co@0.2gNiCoTe₂-240 electrodes toward OER

Catalysts	Electrolyte	Tafel slope (mV dec ⁻¹)	J _{geo} (Current density in mA cm ⁻² @overpotential in mV)	Reference
Co@0.2gNiCoTe ₂ -240	1.0M KOH	34	10@η=280	This work
Co@CoTe ₂ -240		42	10@η=330	
bare Co foam		61	10@η=480	
Co@CoTe ₂	1.0M KOH	42	10@η=286	<i>Inorg. Chem. Front.</i> 7 (2020), 2523-2532.
Ni ₃ Te ₂ -CoTe	1.0M KOH	68	10@η=310	<i>Applied. Surface. Science</i> , 490(2019), 516-521.
Fe-CoTe	1.0M KOH	44	10@η=290	<i>Electrochimica Acta</i> , 321 (2019), 134656.
CoVP@CC	1.0M KOH	55	10@η=380	<i>J. Alloys Compd.</i> 846 (2020),156350
Ni-P	1.0M KOH	110	10@η=415	<i>J. Alloys Compd</i> 847 (2020), 156514
Co-P		114	10@η=431	
Ni ₁ Co ₁ -P		77	10@η=343	
Ni-Co ₃ SeO ₄ /rGo	1.0M KOH	71	10@η=284	<i>Nanoscale</i> , 3 (2021), 3698-3708.
Co _{0.13} Ni _{0.87} Se ₂ /Ti	1.0M KOH	94	100@η=320	<i>Nanoscale</i> , 8 (2016), 3911-3915.
8 mmol NiCoSe	1.0M KOH	102	10@η=280	<i>Cryst. Eng. Comm</i> , 23 (2021), 69–81.
NiCoSe ₂ nanorods	1.0M KOH	64.6	10@η=288	<i>Science Bulletin</i> , 62 (2017) 1373–1379.
NiCoSe ₂ nanosheets		79.5	10@η=290	
NiCo - LDH/NF		102	10@η=330	
Fe-CoS ₂ /CC	1.0M KOH	128	10@η=302	<i>Chemical. Communication</i> , 55 (2019), 2469-2472.
(Co,0.3Ni)-HMT	1.0M KOH	66	10@η=330	<i>Journal. of Energy. Chemistry</i> , 53 (2021), 251-259.